

Communication

Synthesis, Structure, and Magnetic Properties of New Spin Crossover Fe(II) Complexes Forming Short Hydrogen Bonds with Substituted Dicarboxylic Acids

Takumi Nakanishi and Osamu Sato *

Institute for Materials Chemistry and Engineering, Kyushu University, 744 Motoka, Nishi-ku, Fukuoka 8190395, Japan; nakanishi.t.669@s.kyushu-u.ac.jp

* Correspondence: sato@cm.kyushu-u.ac.jp; Tel.: +80-92-802-6208; Fax: +81-92-802-6205

Academic Editor: Helmut Cölfen

Received: 14 August 2016; Accepted: 6 October 2016; Published: 13 October 2016

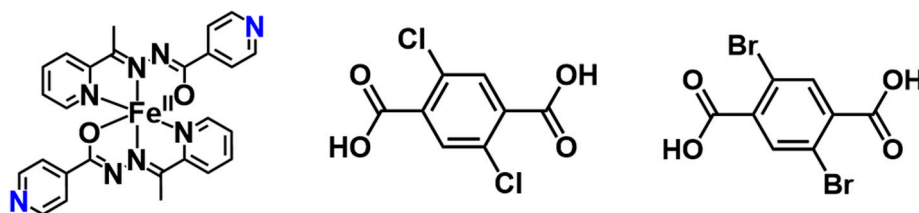
Abstract: We synthesized new Fe(II) compounds consisting of $[\text{Fe}(\text{L})_2]$ (HL: 2-Acetylpyridine isonicotinoylhydrazone) and dicarboxylic acids. Single crystal analysis shows that short hydrogen bonds are formed between $[\text{Fe}(\text{L})_2]$ and dicarboxylic acids. The hydrogen bonding interactions between metal complexes and dicarboxylic acids are complemented by π - π interactions, forming two-dimensional network structures. Magnetic properties show that the Fe(II) compounds exhibit gradual spin crossover behavior around room temperature and a $T_{1/2}$ value is dependent on the halogen substituent on the dicarboxylic acids.

Keywords: spin crossover; hydrazone complex; hydrogen bond

1. Introduction

Hydrogen bonding plays an important role in various biological [1], catalytic [2] and crystal engineering systems [3]. Proton transfer or proton migration between the two components that make up a hydrogen bonding system is an important mechanism of ferroelectricity [4–6]. Furthermore, switching of the conduction and magnetic properties of organic conductor crystals via deuterium transfer in a short hydrogen bond was recently reported [7]; however, although several interesting short hydrogen bonding systems have been reported in pure organic systems, it is still a challenge to construct short hydrogen bonding in functional coordination compounds such as in spin crossover (SCO) and valence tautomeric complexes. There are numerous reports on SCO compounds forming hydrogen bonding networks between anions or solvent molecules and SCO complexes, and these investigations demonstrated that the strength and dimensionality of the hydrogen bonding network contribute to SCO behavior, including the sharpness and hysteresis of the crossover; however, the hydrogen bonding distances in these compounds tend to be long because the $\text{p}K_{\text{a}}$ values of anions or solvent molecules tend to be much higher or lower than the $\text{p}K_{\text{a}}$ value at a proton acceptor site. Therefore, for the construction of short hydrogen bonds, it is important to introduce proton donor or acceptor molecules that have $\text{p}K_{\text{a}}$ values near that of the SCO complex. In this study, we have investigated a new SCO compound comprising an Fe(II) complex and a polyprotic organic acid, wherein a short hydrogen bond is formed between the Fe(II) complex and the polyprotic organic acid. There are few studies that report the crystal structure of SCO compounds with the polyprotic organic acids [8]. Here, 2-Acetylpyridine isonicotinoylhydrazone (HL) was used as a ligand for the Fe(II) complex. The neutral Fe(II) complex bearing this ligand has a proton acceptor site at the terminal Py ring (Scheme 1). Neutral complexes with similar ligands have been reported to exhibit SCO behavior [9,10]. Thus, it was expected that co-crystals comprising the neutral Fe(II) complex and a polyprotic organic acid would also exhibit SCO behavior. We focus on a group of polyprotic organic

dicarboxylic acids, particularly those with halogen substituents. In the SCO compounds introducing halogen-substituted dicarboxylic acids, the hydrogen bond distance is expected to be controlled by changing the halogen substituent without changing the crystal structure. Therefore, $T_{1/2}$ is also expected to be controlled by changing the halogen substituent in dicarboxylic acid. Notably, it has been reported that the $T_{1/2}$ value can be controlled by modifying ligands and exchanging counter-ions in SCO compounds [11,12]. To confirm this hypothesis, 2,5-dichloroterephthalic acid (H_2Cl_2 TPA) and 2,5-dibromoterephthalic acid (H_2Br_2 TPA) were chosen as a counterpart of the hydrogen bond, where the carboxyl group in H_2Cl_2 TPA and H_2Br_2 TPA would act as the proton donor.



Scheme 1. Schematic of proton acceptor complex $[Fe(L)_2]$ and proton donor acids H_2Cl_2 TPA and H_2Br_2 TPA. Proton acceptors on the terminal pyridine ring of 2-acetylpyridine isonicotinoylhydrazone are shown in blue.

2. Results and Discussion

Experiment

The new SCO Fe(II) compounds **1-Cl** and **1-Br** containing H_2Cl_2 TPA and H_2Br_2 TPA, respectively, and 2-acetylpyridine isonicotinoylhydrazone as a ligand were synthesized using the procedure described in the Experimental Section. The newly synthesized **1-Cl** and **1-Br** were characterized using X-ray crystal structure analysis, IR spectroscopy, and magnetic property measurements.

The crystal structures of **1-Cl** and **1-Br** were measured at 123 K and 320 K. The asymmetric unit and molecular arrangement of **1-Cl** are displayed in Figure 1a,b, respectively. The crystal structures of **1-Cl** and **1-Br** are isostructural. Crystallographic data and tables of bond distances and angles for **1-Cl** and **1-Br** are listed in Table 1. The Fe(II)–N and Fe(II)–O coordination distances in **1-Cl** and **1-Br** at 123 K were 1.947(3)–1.966(3) Å and 1.989(2)–1.999(2) Å, respectively, which were consistent with those of low-spin Fe(II) complexes [9]. These coordination distances were found to increase with the increase in temperature, indicating that both **1-Cl** and **1-Br** exhibit SCO. However, the distances observed at 320 K were not equal to those expected to be achieved by high-spin Fe(II) complexes; therefore, SCO in both **1-Cl** and **1-Br** was not completed at 320 K. The crystal structural data measured at 320 K was not sufficient to determine the position of the hydrogen atom involved in hydrogen bond determination from the difference Fourier map. The Fe(II)–N and Fe(II)–O coordination distances in **1-Cl** were observed to be larger than those in **1-Br** at 320 K because **1-Cl** has a higher rate of high-spin iron(II) than that of **1-Br** at this temperature. As shown in Figure 1a, the asymmetric unit of **1-Cl** comprises one Fe(II) complex and one H_2Cl_2 TPA molecule. The molecular arrangement shows that a zig-zag chain was formed with an alternating arrangement of Fe(II) complexes and H_2Cl_2 TPA molecules via hydrogen bonds formed between the N atom in the terminal Py ring in the Fe(II) complex and a carboxyl group in H_2Cl_2 TPA (Figure 1b). The $N4 \cdots O3$ hydrogen bond distance in the terminal pyridine ring was relatively long ($N4 \cdots O3 = 2.663$ Å), whereas the $N8 \cdots O5$ hydrogen bond distance was relatively short ($N8 \cdots O5 = 2.552$ Å) at 123 K. The $N4 \cdots O3$ and $N8 \cdots O5$ hydrogen bond distances in **1-Br** were slightly longer ($N4 \cdots O3 = 2.681$ Å, $N8 \cdots O5 = 2.560$ Å) than those in **1-Cl** at 123 K. The $N8 \cdots O5$ bond distances in **1-Cl** and **1-Br** were short for a N \cdots O-type hydrogen bond but slightly longer than those commonly observed in organic compounds that exhibit proton migration induced by temperature change [13–15]. Regarding the temperature dependency of hydrogen bond distances, studies have reported that the hydrogen bond distance between the Py ring in isonicotinic acid hydrazide, a precursor of L, and

the carboxyl group tends to increase with increasing temperature [16–18]. The increment of N4···O3 and N8···O5 bond distances from 123 K to 320 K was observed in **1-Cl** and **1-Br**. In addition, the difference in hydrogen bond distances at 123 K and 300 K in **1-Cl** was found to be larger than that in **1-Br**, suggesting that the spin transition from low spin to high spin contributes to the elongation of hydrogen bond distance in these compounds. The O–H bond distances in the hydrogen bonds show that the hydrogen atoms involved in both the short and long hydrogen bonds were located closer to the H₂Cl₂TPA molecules at 123 K. The C–O bond distances in the carboxyl groups and the C–N–C angles in the terminal Py ring also support the proposition that the hydrogen atoms in the hydrogen bonds were located closer to the H₂Cl₂TPA molecules. At 123 K, the C34–O3 and C27–O5 bond distances were 1.318(4) Å and 1.305(4) Å, respectively, demonstrating that they are single bonds, i.e., C–O. On the other hand, the C34–O4 and C27–O6 bond distances were 1.210(4) Å and 1.217(4) Å, respectively, indicating that these are double bonds, i.e., C=O. The C–O bond distances were consistent with those found in carboxylic acids [19]. Furthermore, the C–N–C angles in the terminal Py rings at 123 K were 117.6(3)° and 118.7(3)° for C13–N4–C11 and C24–N8–C26, respectively, which were in good agreement with the angle characteristics of a non-protonated Py ring [19]. The same metrical parameters are also present in **1-Br**. These results were consistent with the hydrogen atom positions determined from the difference Fourier map. In addition, similar tendencies of C=O and C–O distances and C–N–C angles as observed at 123 K in **1-Cl** and **1-Br** were found at 320 K, suggesting that the hydrogen atom positions involved in forming the hydrogen bond do not significantly change according to SCO; substantial proton transfer from the carboxyl group to the Py ring does not occur. Thus, **1-Cl** and **1-Br** represent a co-crystal comprising a neutral Fe(II) complex and a neutral acid rather than an ionic crystal. Furthermore, the terminal Py ring with N4 atom in [Fe(L)₂] forms π - π interactions with the H₂Cl₂TPA and H₂Br₂TPA molecules and these distances are 3.363 Å and 3.299 Å, respectively (Figure 2). Overall, **1-Cl** and **1-Br** form a two-dimensional network structure; one-dimensional hydrogen bond chains interact through π - π interactions, forming a two-dimensional structure.

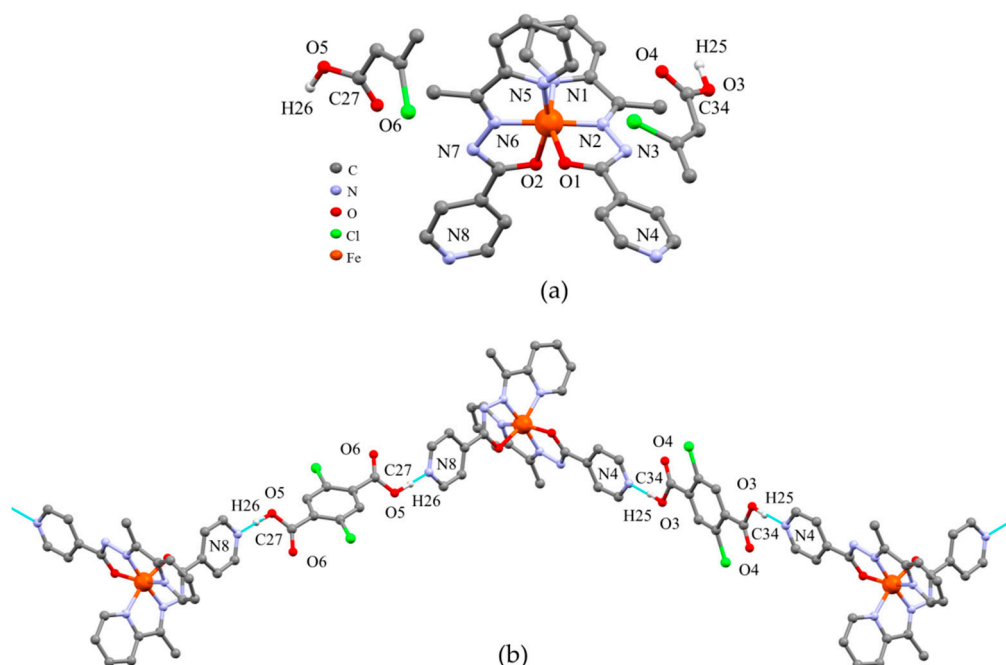


Figure 1. (a) Asymmetric unit of **1-Cl**; (b) Molecular arrangements of [Fe(L)₂] and H₂Cl₂TPA in zig-zag hydrogen bonded chain.

Table 1. Crystallographic data and coordination distances and angles around Fe(II) and the proton donor and acceptor sites, and the hydrogen bond geometry for **1-Cl** and **1-Br** at 123 K and 320 K.

Crystallographic Data				
	1-Cl		1-Br	
Formula	C ₃₄ H ₂₆ Cl ₂ FeN ₈ O ₆		C ₃₄ H ₂₆ Br ₂ FeN ₈ O ₆	
Formula weight	769.38		858.28	
Crystal system	Triclinic		Triclinic	
T (K)	123	320	123	320
Space group	P-1		P-1	
<i>a</i> (Å)	8.336(3)	8.1849(16)	8.3141(12)	8.2936(18)
<i>b</i> (Å)	8.606(3)	8.6570(17)	8.7502(14)	8.7689(15)
<i>c</i> (Å)	23.279(8)	23.026(5)	23.465(4)	24.150(4)
α (°)	99.212(9)	97.818(5)	77.589(8)	77.177(11)
β (°)	97.935(8)	98.149(10)	82.085(10)	81.980(10)
γ (°)	91.648(7)	91.536(6)	87.203(10)	87.835(13)
<i>V</i> (Å ³)	1630.60(10)	1667.7(6)	1651.0(4)	1695.7(5)
<i>Z</i>	2		2	
Dcal (g/cm ³)	1.563	1.528	1.726	1.681
<i>F</i> (000)	855	784	860	860
Data collected	27257	28574	29119	29629
Unique data	7389	7590	7545	7715
<i>R</i> (int)	0.0499	0.0500	0.0672	0.0687
GOF on <i>F</i> ²	1.131	1.160	1.084	1.146
<i>R</i> ₁ [<i>I</i> > 2σ(<i>I</i>)]	0.0600	0.0733	0.0463	0.0738
Bond Lengths (Å) and Angles (°)				
	1-Cl (123 K)	1-Cl (320 K)	1-Br (123 K)	1-Br (320 K)
Fe1–N1	1.966(3)	2.077(4)	1.959(3)	2.011(4)
Fe1–N2	1.878(2)	1.989(3)	1.873(2)	1.923(4)
Fe1–O1	1.999(2)	2.047(3)	1.991(2)	2.010(3)
Fe1–N5	1.947(3)	2.089(3)	1.943(3)	1.974(4)
Fe1–N6	1.879(2)	1.988(4)	1.869(3)	1.916(4)
Fe1–O2	1.989(2)	2.043(3)	1.991(2)	2.016(4)
C34–O3	1.318(4)	1.315(4)	1.316(4)	1.306(7)
C34–O4	1.210(4)	1.187(6)	1.204(4)	1.173(6)
C27–O5	1.305(4)	1.299(5)	1.302(4)	1.312(6)
C27–O6	1.217(4)	1.208(5)	1.212(4)	1.199(6)
C13–N4–C11	117.6(3)	116.6(4)	117.3(3)	115.8(5)
C24–N8–C26	118.7(3)	118.3(3)	117.9(3)	117.7(5)
Hydrogen Bond Geometries (Å, °)				
N4–O3	2.663(4)	2.692(5)	2.681(4)	2.694(4)
N8–O5	2.552(4)	2.574(4)	2.560(4)	2.578(4)
O3–H25	1.03(7)	–	0.82(4)	–
N4–H25	1.64(7)	–	1.86(4)	–
O5–H26	1.09(6)	–	1.04(7)	–
N8–H26	1.47(6)	–	1.52(7)	–
N4–H25–O3	174(6)	–	177(4)	–
N8–H26–O5	175(6)	–	173(6)	–

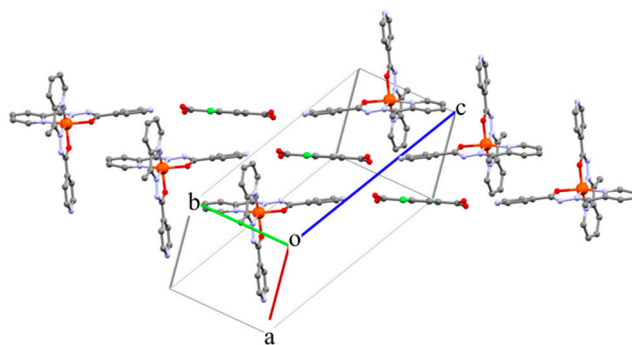


Figure 2. The π - π interaction between $[\text{Fe}(\text{L})_2]$ and $\text{H}_2\text{Cl}_2\text{TPA}$ in **1-Cl**.

The IR spectra of **1-Cl** and **1-Br** also support the proposal that both compounds are co-crystals (Figure 3a,b). It is known that the broad peaks derived from $\text{O}-\text{H}\cdots\text{N}$ stretching appear around 1950 and 2450 cm^{-1} when strong hydrogen bonds are present in the crystal [20]. However, the peak around 1950 cm^{-1} shifts toward 2150 cm^{-1} if the proton is located on the N side of the hydrogen bond, i.e., $\text{O}\cdots\text{H}-\text{N}$ [21]. Furthermore, $\text{C}=\text{O}$ stretching in the carboxyl group has been utilized to differentiate between the protonated and deprotonated state of the carboxyl group; for example, in terephthalic acid, $\text{C}=\text{O}$ stretching appeared at 1692 cm^{-1} , whereas in disodium terephthalate, $\text{C}=\text{O}$ stretching appeared at 1567 cm^{-1} . The IR spectra of **1-Cl** and **1-Br** show broad peaks at around 1950 and 2450 cm^{-1} , and strong peaks at 1713 cm^{-1} and 1717 cm^{-1} , similar to those observed for $\text{H}_2\text{Cl}_2\text{TPA}$ (Figure 3a, gray line) and $\text{H}_2\text{Br}_2\text{TPA}$ (Figure 3b, gray line), respectively. The IR data indicate that these compounds contain a neutral $\text{Fe}(\text{II})$ complex and neutral $\text{H}_2\text{Cl}_2\text{TPA}$ and $\text{H}_2\text{Br}_2\text{TPA}$, respectively.

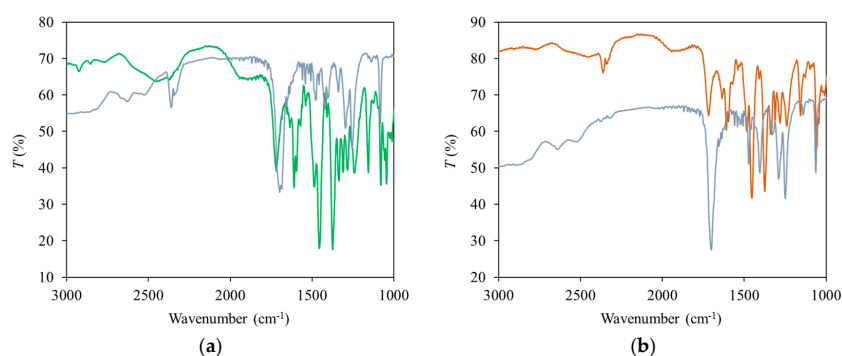


Figure 3. (a) IR spectra for **1-Cl** (green line) and $\text{H}_2\text{Cl}_2\text{TPA}$ (gray line); (b) IR spectra for **1-Br** (brown line) and $\text{H}_2\text{Br}_2\text{TPA}$ (gray line).

Magnetic susceptibility measurements for **1-Cl** and **1-Br** were performed over the temperature range of 10 – 400 K at a sweep rate of $1\text{ K}\cdot\text{min}^{-1}$ with a magnetic field of 5 kOe . The $\chi_m T$ - T plots of **1-Cl** and **1-Br** in Figure 4 show that both compounds exhibited gradual spin crossover. In the low-spin state, the $\chi_m T$ values in **1-Cl** and **1-Br** were nearly zero, which was in good agreement with the expected value for low-spin $\text{Fe}(\text{II})$ ($S = 0$). Upon warming, the $\chi_m T$ value of **1-Cl** gradually increased above 210 K and reached $2.49\text{ cm}^3\cdot\text{K}\cdot\text{mol}^{-1}$ at 400 K , whereas the $\chi_m T$ value of **1-Br** gradually increased above 250 K and reached $1.90\text{ cm}^3\cdot\text{K}\cdot\text{mol}^{-1}$ at 400 K . These values were less than the expected value for high-spin $\text{Fe}(\text{II})$ ($S = 2$) because the spin crossover was not complete even at 400 K . The $\chi_m T$ values in **1-Cl** and **1-Br** at 320 K are $1.60\text{ cm}^3\cdot\text{K}\cdot\text{mol}^{-1}$ and $0.53\text{ cm}^3\cdot\text{K}\cdot\text{mol}^{-1}$, respectively. This indicates that 53% and 18% of low-spin $\text{Fe}(\text{II})$ changed to high-spin $\text{Fe}(\text{II})$, respectively, in **1-Cl** and **1-Br** at 320 K . The difference of the fraction of high-spin $\text{Fe}(\text{II})$ between **1-Cl** and **1-Br** at 320 K could also be followed from the result in the single-crystal X-ray measurement that showed the $\text{Fe}(\text{II})-\text{N}$ and $\text{Fe}(\text{II})-\text{O}$ coordination distances for **1-Cl** are larger than those for **1-Br** at 320 K . The difference in $T_{1/2}$ between

1-Cl (314 K) and **1-Br** (376 K) indicates that changing the halogen substituent on the dicarboxylic acids can influence the hydrogen bond distance and the SCO behavior without changing the molecular arrangement; however, these compounds do not exhibit abrupt SCO despite the presence of short hydrogen bonds, caused by the low dimensionality of the hydrogen bonding network.

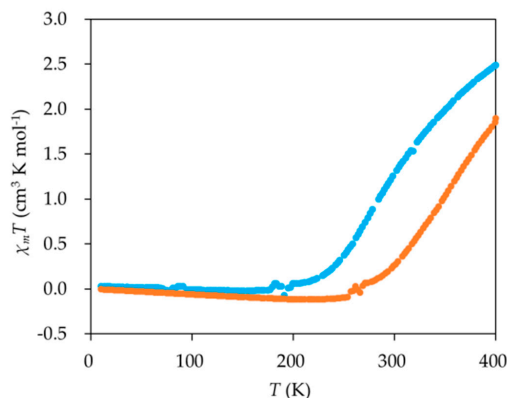


Figure 4. $\chi_m T$ - T plots for **1-Cl** (blue dots) and **1-Br** (brown dots).

3. Experimental Section

3.1. Synthesis

3.1.1. Synthesis of Ligand HL

HL was synthesized according to the method described by Musuc et al. [22].

3.1.2. Synthesis of [Fe(L)₂](H₂Cl₂TPA) (**1-Cl**)

HL (48 mg, 0.20 mmol) was dissolved in methanol (30 mL), and FeSO₄·7H₂O (27 mg, 0.10 mmol) was added to the solution. The mixture was stirred for 30 min. Following this, H₂Cl₂TPA (23.5 mg, 0.10 mmol) was added and the mixture was stirred for 30 sec. Subsequently, the solution was evaporated using a N₂ gas flow over several days. Plate shape crystals were obtained (47 mg, 61%). Elemental analysis calcd for C₃₄H₂₄Cl₂FeN₈O₆ (769.38); C 53.08, H 3.41, N 14.56; found. C 52.66, H 3.54, 14.50.

3.1.3. Synthesis of [Fe(L)₂](H₂Br₂TPA) (**1-Br**)

The synthetic procedure for **1-Br** is similar to that for **1-Cl** except for the use of H₂Br₂TPA instead of H₂Cl₂TPA. Plate shape crystals were obtained by evaporation of the solution containing HL, FeSO₄·7H₂O and H₂Br₂TPA using a N₂ gas flow over several days (65 mg, 76%). Elemental analysis calcd for C₃₄H₂₄Br₂FeN₈O₆ (858.28); C 47.58, H 3.05, N 13.06; found. C 47.66, H 3.10, 12.85.

3.2. X-ray Structure Determination

Diffraction data of **1-Cl** and **1-Br** at 123 K and 320 K was collected on a Rigaku charge-coupled device (CCD) diffractometer (Rigaku, Tokyo, Japan). A crystal was glued onto a nylon loop and enveloped in a temperature-controlled steam (Rigaku, Tokyo, Japan) of dry N₂ gas during data collection. The structures were solved by direct methods and refined with full-matrix least-squares procedures using the program SHELXS-97 [23]. Hydrogen atoms involved in hydrogen bonds were determined from Fourier Difference Map at 123 K. Other hydrogen atoms were determined by calculation and refined using the riding model. All non-hydrogen atoms were refined anisotropically. CCDC 1487718 (**1-Cl** 123 K), 1506004 (**1-Cl** 320 K), 1497560 (**1-Br** 123 K) and 1506005 (**1-Br** 320 K) contains the supplementary crystallographic data for this paper. These data can be obtained free of

charge via <http://www.ccdc.cam.ac.uk/conts/retrieving.html> (or from the CCDC, 12 Union Road, Cambridge CB2 1EZ, UK; Fax: +44 1223 336033; E-mail: deposit@ccdc.cam.ac.uk).

3.3. IR Spectra

IR spectra were recorded with KBr pellet sample by a JASCO FT/IR-660 Plus spectrometer (JASCO, Tokyo, Japan) in the 600–4000 cm^{-1} region.

3.4. Magnetic Property Measurement

Magnetic measurements were performed on a Quantum Design MPMS-5S SQUID (superconducting quantum-interference device) magnetometer (Quantum Design, San Diego, CA, USA), and data were corrected for the diamagnetic contribution, calculated from Pascal's constants.

4. Conclusions

In summary, we have synthesized a new SCO complex $[\text{Fe}(\text{L})_2]$ that can form short hydrogen bonds with a dicarboxylic acid. The crystal structures of **1-Cl** and **1-Br** showed that a zig-zag hydrogen-bonded chain was formed between the terminal Py ring in the Fe complex and the carboxyl group in $\text{H}_2\text{Cl}_2\text{TPA}$ and $\text{H}_2\text{Br}_2\text{TPA}$. Two different hydrogen bond distances were observed; one was long, whereas the other was short, and these distances in **1-Br** are slightly longer than in **1-Cl**. Both short hydrogen bond distances are attributed to $\text{N}\cdots\text{O}$ -type hydrogen bonds and are slightly longer than those for organic compounds reporting the proton migration phenomenon. The dependence of hydrogen bond distances on temperature was observed to be similar to that in organic compounds comprising isonicotinic acid hydrazide and dicarboxylic acids. Furthermore, the spin transition from low-spin to high-spin state was stated to contribute to the elongation of hydrogen bond distances in **1-Cl** and **1-Br**. O–H and C–O bond distances in the carboxyl group and the C–N–C angle in the terminal Py rings suggested that the hydrogen atoms involved in the hydrogen bonds are localized on the carboxyl group in $\text{H}_2\text{Cl}_2\text{TPA}$ and $\text{H}_2\text{Br}_2\text{TPA}$. The IR spectra of **1-Cl** and **1-Br**, in particular the presence of an O–H \cdots N stretching mode, also supported the fact that the hydrogen atoms are located on the carboxyl group. This indicated that **1-Cl** and **1-Br** are co-crystals comprising neutral $[\text{Fe}(\text{L})_2]$ and $\text{H}_2\text{Cl}_2\text{TPA}$ and $\text{H}_2\text{Br}_2\text{TPA}$. Magnetic measurements for **1-Cl** and **1-Br** showed that a gradual SCO occurred around room temperature, and it was confirmed that the $T_{1/2}$ value in SCO compounds comprising halogen-substituted dicarboxylic acids can be influenced by only changing the halogen substituent without changing the molecular arrangement.

Author Contributions: Takumi Nakanishi and Osamu Sato have designed the compounds and performed any experiment and analysis.

Conflicts of Interest: The authors declare no conflict of interest.

References

1. Yamaguchi, S.; Kamikubo, H.; Kurihara, K.; Kuroki, R.; Niimura, N.; Shimizu, N.; Yamazaki, Y.; Kataoka, M. Low-barrier hydrogen bond in photoactive yellow protein. *Proc. Natl. Acad. Sci. USA* **2009**, *106*, 440–444. [[CrossRef](#)] [[PubMed](#)]
2. Ohshima, T.; Shibuguchi, T.; Fukuta, Y.; Shibasaki, M. Catalytic asymmetric phase-transfer reactions using tartrate-derived asymmetric two-center organocatalysts. *Tetrahedron* **2004**, *60*, 7743–7754. [[CrossRef](#)]
3. Shan, N.; Bond, A.D.; Jones, W. Crystal engineering using 4,4'-bipyridyl with di- and tricarboxylic acids. *Cryst. Eng.* **2002**, *5*, 9–24. [[CrossRef](#)]
4. Horiuchi, S.; Ishii, F.; Kumai, R.; Okimoto, Y.; Tachibana, H.; Nagaosa, N.; Tokura, Y. Ferroelectricity near room temperature in co-crystals of nonpolar organic molecules. *Nat. Mater.* **2005**, *4*, 163–166. [[CrossRef](#)] [[PubMed](#)]
5. Horiuchi, S.; Kumai, R.; Tokura, Y. A supramolecular ferroelectric realized by collective proton transfer. *Angew. Chem. Int. Ed. Engl.* **2007**, *46*, 3497–3501. [[CrossRef](#)] [[PubMed](#)]

6. Sato, O. Dynamic molecular crystals with switchable physical properties. *Nat. Chem.* **2016**, *8*, 644–656. [[CrossRef](#)] [[PubMed](#)]
7. Ueda, A.; Yamada, S.; Isono, T.; Kamo, H.; Nakao, A.; Kumai, R.; Nakao, H.; Murakami, Y.; Yamamoto, K.; Nishio, Y.; et al. Hydrogen-bond-dynamics-based switching of conductivity and magnetism: A phase transition caused by deuterium and electron transfer in a hydrogen-bonded purely organic conductor crystal. *J. Am. Chem. Soc.* **2014**, *136*, 12184–12192. [[CrossRef](#)] [[PubMed](#)]
8. Coronado, E.; Gimenez-Lopez, M.C.; Gimenez-Saiz, C.; Romero, F.M. Spin crossover complexes as building units of hydrogen-bonded nanoporous structures. *CrystEngComm* **2009**, *11*, 2198–2203. [[CrossRef](#)]
9. Hill, S.; Datta, S.; Liu, J.; Inglis, R.; Milios, C.J.; Feng, P.L.; Henderson, J.J.; del Barco, E.; Brechin, E.K.; Hendrickson, D.N. Magnetic quantum tunneling: Insights from simple molecule-based magnets. *Dalton Trans.* **2010**, *39*, 4693–4707. [[CrossRef](#)] [[PubMed](#)]
10. Zhang, L.; Xu, G.C.; Xu, H.B.; Zhang, T.; Wang, Z.M.; Yuan, M.; Gao, S. Abrupt spin transition around room temperature and light induced properties in Fe(II) complexes with N₄O₂ coordination sphere. *Chem. Commun.* **2010**, *46*, 2554–2556. [[CrossRef](#)] [[PubMed](#)]
11. Paulsen, H.; Duelund, L.; Zimmermann, A.; Averseng, F.; Gerdan, M.; Winkler, H.; Toftlund, H.; Trautwein, A.X. Substituent effects on the spin-transition temperature in complexes with tris(pyrazolyl) ligands. *Monatsh. Chem.* **2003**, *134*, 295–306. [[CrossRef](#)]
12. Lemerrier, G.; Brefuel, N.; Shova, S.; Wolny, J.A.; Dahan, F.; Verelst, M.; Paulsen, H.; Trautwein, A.X.; Tuchagues, J.P. A range of spin-crossover temperature $T_{1/2} > 300$ K results from out-of-sphere anion exchange in a series of ferrous materials based on the 4-(4-imidazolylmethyl)-2-(2-imidazolylmethyl)imidazole (trim) ligand, [Fe(trim)₂]₂X₂ (X = F, Cl, Br, I): Comparison of experimental results with those derived from density functional theory calculations. *Chem. Eur. J.* **2006**, *12*, 7421–7432. [[PubMed](#)]
13. Cowan, J.A.; Howard, J.A.; McIntyre, G.J.; Lo, S.M.; Williams, I.D. Variable-temperature neutron diffraction studies of the short, strong hydrogen bonds in the crystal structure of pyridine-3,5-dicarboxylic acid. *Acta Crystallogr. B* **2005**, *61*, 724–730. [[CrossRef](#)] [[PubMed](#)]
14. Steiner, T.; Majerz, I.; Wilson, C.C. First O–H–N hydrogen bond with a centered proton obtained by thermally induced proton migration. *Angew. Chem. Int. Ed.* **2001**, *40*, 2651–2654. [[CrossRef](#)]
15. Cowan, J.A.; Howard, J.A.K.; McIntyre, G.J.; Lo, S.M.F.; Williams, I.D. Variable-temperature neutron diffraction studies of the short, strong n center dot center dot center dot o hydrogen bonds in the 1:2 co-crystal of benzene-1,2,4,5-tetracarboxylic acid and 4,4'-bipyridyl. *Acta Crystallogr. Sect. B-Struct. Sci.* **2003**, *59*, 794–801. [[CrossRef](#)]
16. Grobelny, P.; Mukherjee, A.; Desiraju, G.R. Drug-drug co-crystals: Temperature-dependent proton mobility in the molecular complex of isoniazid with 4-aminosalicylic acid. *CrystEngComm* **2011**, *13*, 4358–4364. [[CrossRef](#)]
17. Cherukuvada, S.; Nangia, A. Fast dissolving eutectic compositions of two anti-tubercular drugs. *CrystEngComm* **2012**, *14*, 2579–2588. [[CrossRef](#)]
18. Aitipamula, S.; Wong, A.B.H.; Chow, P.S.; Tan, R.B.H. Novel solid forms of the anti-tuberculosis drug, isoniazid: Ternary and polymorphic cocrystals. *CrystEngComm* **2013**, *15*, 5877–5887. [[CrossRef](#)]
19. Bis, J.A.; Zaworotko, M.J. The 2-aminopyridinium-carboxylate supramolecular heterosynthon: A robust motif for generation of multiple-component crystals. *Cryst. Growth Des.* **2005**, *5*, 1169–1179. [[CrossRef](#)]
20. Bhunia, M.K.; Das, S.K.; Bhaumik, A. Temperature induced proton transfer in a hydrogen bonded supramolecule. *Chem. Phys. Lett.* **2010**, *498*, 145–150. [[CrossRef](#)]
21. Aakeröy, C.B.; Hussain, I.; Forbes, S.; Desper, J. Exploring the hydrogen-bond preference of N–H moieties in co-crystals assembled via O–H(acid)⋯N(py) intermolecular interactions. *CrystEngComm* **2007**, *9*, 46–54. [[CrossRef](#)]
22. Ababei, L.V.; Kriza, A.; Andronesu, C.; Musuc, A.M. Synthesis and characterization of new complexes of some divalent transition metals with 2-acetyl-pyridyl-isonicotinoylhydrazone. *J. Therm. Anal. Calorim.* **2011**, *107*, 573–584. [[CrossRef](#)]
23. Sheldrick, G.M. A short history of SHELX. *Acta Cryst. A* **2008**, *A64*, 112–122. [[CrossRef](#)] [[PubMed](#)]

